い．コラーゲンは如何にして蓄積されるのだろうか．コラーゲンは29種の型に分類されるスーパーファミリーを形成しており，46のα鎖遺伝子が確認されているが，組織線維化に関係するのは線維性コラーゲンであるⅠ，Ⅲ，Ⅴ型コラーゲンであり，その中でも線維を構築する過程で果たす役割が異なっている[1]．Ⅰ型は最も多い成分で組織線維症の“主犯”として捉えられている．図1に一般的な線維性コラーゲンの各α鎖と呼ばれる遺伝子が，コラーゲンドメインであるGly-X-Yモチーフにより3重らせん構造のトリマー分子となり，それらが細胞外でプロセスを受けた後に自己会合して束を形成することで“コラーゲン線維”が形成されていくという過程を示す．正常組織のコラーゲン線維を電子顕微鏡で観察すると，真皮や腱の様に，直径100nmを超える線維が規則的に張り巡らされている組織もあれば，直径10数nm程の細かい線維が分岐して緩く敷き詰められ，細胞の生育環境を形成している組織もあり，バリエーションに富んでいる．これらの細胞外環境の違いはコラーゲンの線維束の組まれ方によってもたらされ，当該組織の機能と密接に関係している．太い線維でも細いものでも主成分はⅠ型コラーゲンであるが，Ⅲ型とⅤ型は形成途中の細いコラーゲンに，より多く含まれる．特にⅤ型α1鎖はN末にテロペプチドと呼ばれる特徴的な非コラーゲン領域を有しており（図1C），立体的な制約からⅤ型コラーゲンはコラーゲン線維束の外周部分に配置され，線維の隙間からN末ドメインを突き出す形態をとる（図1D）．このためⅤ型コラーゲン含量が増すと線維径が細くなるとされる．このN末領域の役割は解明されていないが，他のECM分子と相互作用しながらコラーゲン線維の径を調節すると考えられている[2]．またⅤ型α1鎖のKOマウスは，全くコラーゲン線維を形成できず致死となり，線維の形成初期にⅤ型コラーゲンが芯を形成する役割があるとみられる[3]など，線維束の形成機構について重要なヒントを握っているものと考えられる．

我々は線維化におけるコラーゲン線維束の形成と蓄積の過程を追跡したいと考え，マウスの背部皮膚に穴を空け，その欠損部を埋める過程において各種コラーゲン遺伝子の動き，線維芽細胞の動員，コラーゲン線維束の電子顕微鏡レベルでの形態形成を観察する実験を行なった．

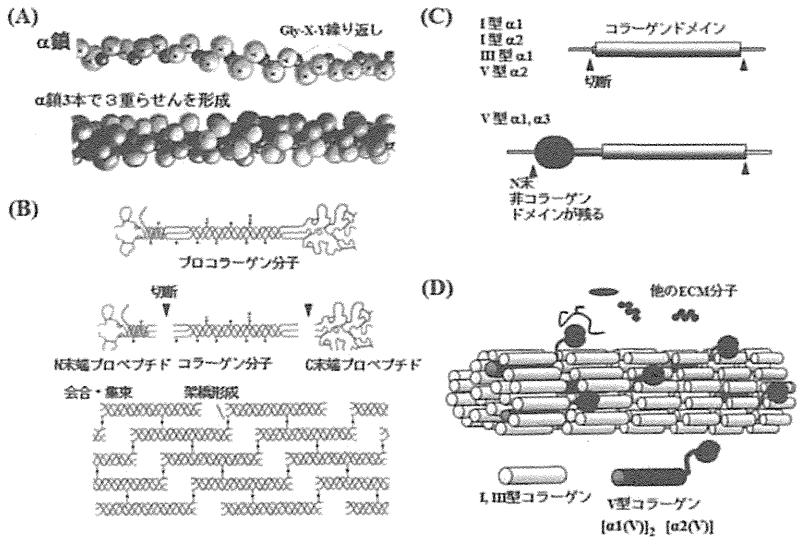

図1　線維性コラーゲンの構造と線維束の構築

（A）コラーゲンドメインのアミノ酸一次構造．Gly-X-Y繰り返し構造と，小さいグリシン残基が縒りあわせの中心となり3重らせん構造を形成するモデルを示す．（Bruce, A. et al.：Molecular Biology of the Cell, Garland Science, 2007より出典）

（B）線維性コラーゲンの会合．分泌直後はプロコラーゲンとしてN，C末のプロペプチドを持つが，細胞外でプロペプチドが切断を受け，成熟コラーゲン分子となり，会合体を形成する．この束が電子顕微鏡で観察されるコラーゲン線維である．（大塚吉兵衛，安孫子宣光著：医歯薬系学生のためのビジュアル生化学・分子生物学（改訂第3版）日本医事新報社，2008より出典）

（C）Ⅰ型，Ⅲ型，Ⅴ型コラーゲンの構造の違い．Ⅰ型，Ⅲ型，Ⅴ型α2鎖はプロペプチドを除くと純粋な3重らせん構造が残るが，Ⅴ型α1鎖とα3鎖はプロペプチド以外にN末に残る非コラーゲンドメイン，テロペプチドを有する構造をしている．

（D）線維性コラーゲンの会合模式図．Ⅰ型，Ⅲ型を基本としてコラーゲンの束が形成される．Ⅴ型コラーゲンはN末のテロペプチドの為，線維の外周部に配置し，他のECM分子とのインタラクションを通じて線維の構築を調節するとされている．

(Lynsenmayer, T. F. et al. J. Cell Biol 1993.（文献2）より改変)

3．実験結果１：各種コラーゲン遺伝子の発現と治癒後のコラーゲン組織

マウスの創傷治癒による創部の再生は，短期間でコラーゲンの新生と線維構築過程を観察する最良のモデルである．マウスの背部皮膚に直径６㎜の全層欠損創を形成し，各種コラーゲン遺伝子の活性化と発現局在を *In situ* hybridization を用いて調べた（図２）．ここで示すコラーゲン遺伝子（Ⅰ型α１，Ⅲ型α１，Ⅴ型α１，α３）は，創傷後４日後から新生肉芽組織を中心に，ほぼ同時に発現し始めた．中でもⅤ型コラーゲンは創傷前には殆ど発現が見られなかったが，創傷

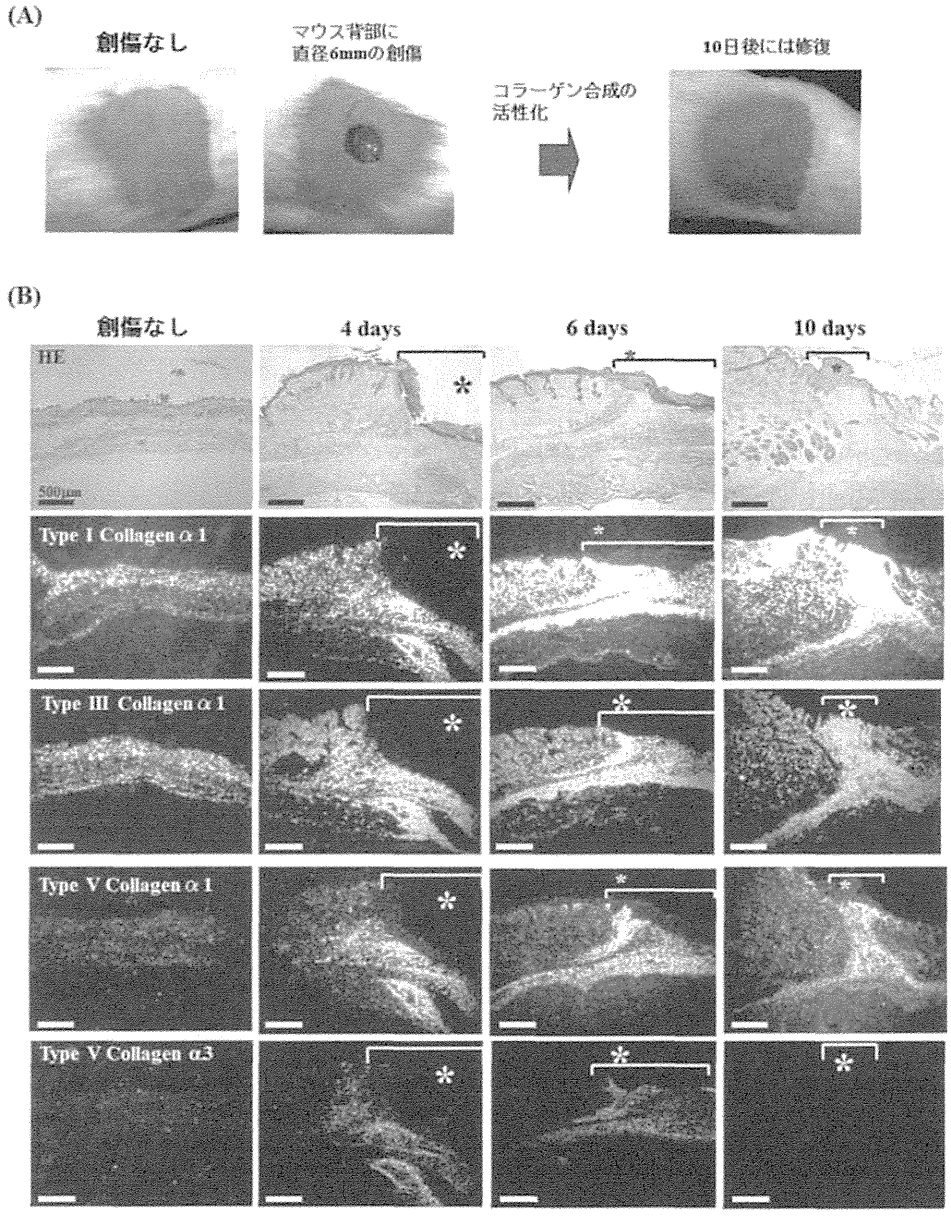

図２　皮膚創傷治癒における各種コラーゲン遺伝子の発現パターン

（A）マウス背部に６㎜の皮膚全層欠損創を形成した外観．10日程で傷は修復される．

（B）創傷部の組織像．左から創傷なし，創傷後４日，６日，10日後の組織像．＊が創傷部分を示す．写真上段からHE染色像，Ⅰ型α１鎖の *In situ* hybridization，同じくⅢ型α１鎖，Ⅴ型α１鎖，Ⅴ型α３鎖の *In situ* を示している．白く見えるシグナルが，各コラーゲン遺伝子の mRNA 発現に対応する．Ⅴ型コラーゲンの方が創部に，より特異的に発現しているのが分かる．Bar は500μm．

(Sumiyoshi, H. et al, Connect. Tissue Res. 2012.（文献４）より改変)

部の領域で急激に発現量が増しており，Ⅰ型より明瞭なコントラストを成していた．この事からも形成中のコラーゲンに，より多くのⅤ型コラーゲンが含まれていることが確認できた．この実験は線維形成に関わるコラーゲン分子種を網羅的に探していく事を目的としており，本来皮膚には発現しないとされるコラーゲン種（Ⅱ型α1，XI型α1ともに陰性）もまた解析を試みた．その中から胎児期の臍帯や羊膜に発現しているが，成体の組織中に通常見られないα3（Ⅴ）が，皮膚創傷治癒事例でのコラーゲン線維形成初期にのみ特異的に発現してくることが見出された．このことについては改めて後述したい．

電子顕微鏡で新生コラーゲンの構築過程を観察すると，創傷部位には細くて方向性がばらばらの，分岐のあるコラーゲン線維①と，太くて規則的に並行する分岐のないコラーゲン線維② が存在し，（図3Ａ）線維化が進むにつれ，太い線維の密度が増していった．しかし創傷部の新生コラーゲンは太いものでも，50nm程であり，真皮コラーゲン線維（100nm以上）の半分である．またコラーゲンの形態にも明らかな違いがあり，真皮コラーゲンはきれいな流紋を示し，多方向に組まれ，表面も滑らかである一方，新生コラーゲンに由来する傷痕部は平板で層状に配列しており表面には真皮にない粗さがあった．線維芽細胞の形態も異なり，真皮線維芽細胞は星形を示すのに対し，傷痕部の線維芽細胞は横長である．このように創傷部に再建された組織は正規のものと異なる構造を持っていた（図3Ｂ）．そのためか傷痕は1年を経過しても明瞭に見分けることが出来た．この線維形態は皮下筋膜の結合組織にみられるコラーゲンの構造と類似している．ここで，創傷部位のHE染色像と *In situ* hybridizationの観察像を再度見直してみると，コラーゲンを強く発現している線維芽細胞の領域は真皮からではなく，皮下と筋膜との境界部結合組織から流れて来るようなパターンが見られる．更に後になって特徴的な発現パターンを示していたコラーゲンα3（Ⅴ）の発現は筋膜由来細胞に特異的であることが示された．

これらの筋膜に存在する細胞はマイルドなコラゲナーゼ処理にて，ほぼ均一な細胞群として単離することが出来た．これらは，細胞骨格に乏しく，多数の空胞をもった，正常筋膜内に多数観察される細胞であるが，これを培養下，血清で活性化したところ，創傷部にみられる充実した粗面小胞体を持ち，アクチンファイバーの発達した細胞に形態変化を起こし，線維産生細胞になることが確認できた（図4）．つまり，皮膚の創傷を埋めたのは本来の皮膚由来である真皮線維芽細胞ではなく，創傷という非常事態に際して活性化し，遊走・増殖してきた筋膜の細胞であり，埋められたコラーゲ

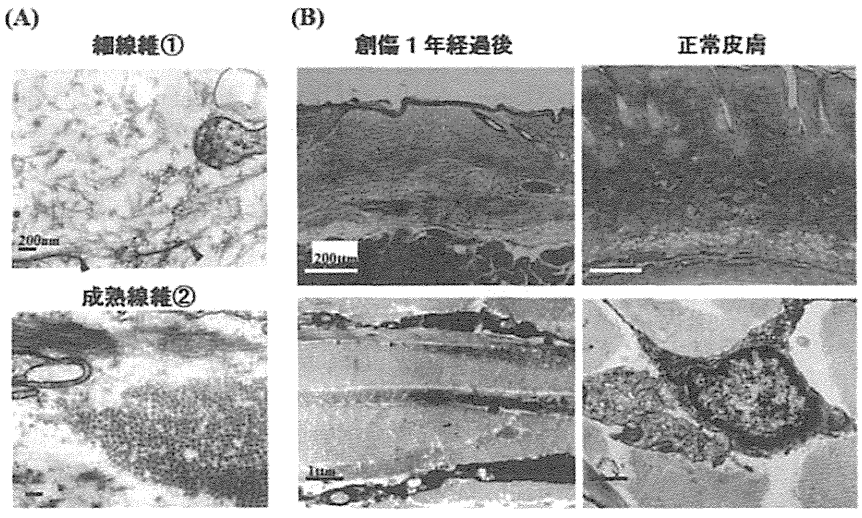

図3　新生コラーゲンにみられる，2種類のコラーゲン線維

(A) 細線維①は直径15nm程のばらついた形状の細い線維．会合・集束しつつある線維もみられる（矢頭）．成熟線維②は直径50nm程で方向も揃った形状を示す．Barは200nm．

(B) 左側：創傷1年後線維瘢痕組織，右側：正常皮膚組織．上段：マッソントリクローム染色．創傷後瘢痕のコラーゲン線維走行は平坦だが，正常真皮は流紋状を示す．Barは200μm．下段：同部位の電子顕微鏡像．創傷後瘢痕のコラーゲンは直径50nm程の水平方向の層構造で，線維芽細胞も横長の形態を示す．正常真皮は直径100nm以上の3次元に張り巡らされた線維で線維芽細胞は星形の形態を示す．Barは1μm．

（住吉秀明，稲垣豊：医学のあゆみ Vol. 244，No 6，医歯薬出版株式会社，2013より出典）

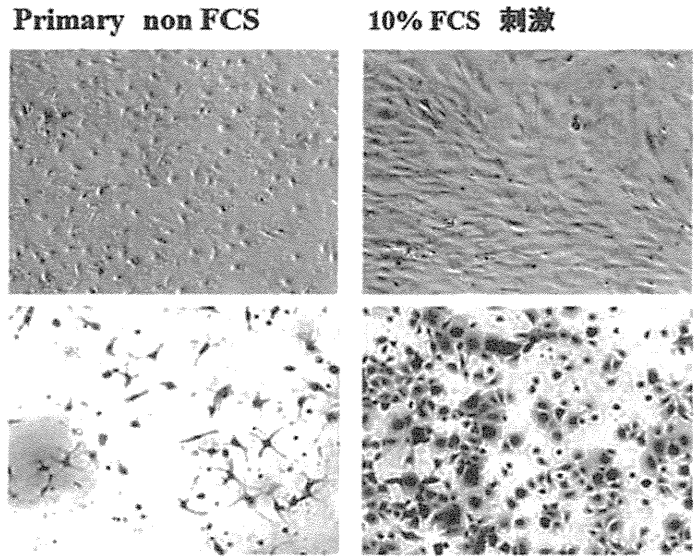

図4 筋膜細胞の初代培養と血清による活性化

左列：単離直後の筋膜細胞，無血清条件．右列：10%血清で刺激した後，継代した筋膜細胞．上段：位相差顕微鏡像．下段：クリスタルバイオレット染色像．単離した直後の筋膜細胞は長い触手をもち，血清なしでは増殖せず形態を保つが，血清を加えて活性化すると細胞は伸展し，活発な増殖を始める．

ンは異所性のリモデリングにより再生されたということが出来る．これらの細胞は静止状態では，ほとんどコラーゲンを産生しないが，刺激を受けると線維産生細胞となる前駆細胞と言えるものであり，肝線維化における星細胞の活性化機構にも通じるものとして興味深い．このことがどんな生体的な意味をもつのかを考察するに，一度出来上がった組織が損傷した際，本来の構成細胞をもって修復することは発生を逆行させる様に難しいことであり，むしろ修復屋といえる準万能細胞を各組織に配置しておいて対応する方が合目的であると考えることが出来る．そして，線維症とは線維産生細胞への活性化が持続するような要因が加わることによる創傷修復過程からの逸脱であると捉えられる．皮膚浅筋膜由来細胞は単離しやすく，線維産生細胞への形質転換モデル細胞として活性化を遮断する薬剤開発にも使えるのではないかと期待している．

4．実験結果2：創傷治癒過程におけるα3（V）鎖の発現について

ここで新たに見出された創傷部のα3（V）鎖の発現について述べる．α3（V）はV型コラーゲン遺伝子の一つであり，成体マウスの組織中にほとんど見られない希少なコラーゲン分子種である．以前から第三のV型コラーゲンα鎖があることが知られていたが，α3（V）遺伝子構造が明らかなったのは近年である[5]．通常のV型コラーゲンはα1鎖2本とα2鎖1本からなるヘテロトリマー［α1（V)］2［α2（V)］でありα3（V）は含まれていない（図1C，D）．α3（V）鎖はα1鎖，α2鎖と共同して［α1（V)］［α2（V)］［α3（V)］の3種ヘテロトリマーを形成し，単独で3重らせんを巻くことはない．α3（V）鎖を含むコラーゲン線維は通常のV型コラーゲンと，この3種トリマーが混在する形になる．α3鎖のN末にもテロペプチドが存在し，α1鎖のN末ドメインが酸性アミノ酸に富むのに対し，α3鎖のN末は塩基性アミノ酸が多く含まれ，全く異なる機能をもつと考えられる．この領域はヘパリン硫酸糖鎖結合ドメインが含まれ，良好な細胞接着性をもつ事が示されている[6]．α3（V）鎖は主に胎児期の臍帯，羊膜，筋膜，骨膜などに局在し，生後には見られなくなる[6]．

この特殊なコラーゲン種が創傷治癒過程に見出され，新生コラーゲンの構築に付与していること，また4日目と6日目に発現があり，10日目以後には，消失してしまう時期特異性があり，発現部位についても筋膜との境界部，真皮との境界部，表皮細胞との境界部等，境をなす部位により多くみられる部位特異性がみられた（図2）．面白いことに，これらのα3（V）鎖が多く発現する領域はコラーゲン線維の会合集束が抑制され，細線維が多く線維密度がルーズである傾向があり，特に皮下組織と筋膜の成すα3（V）鎖の豊富な境界部には剥離面が形成され，癒着が解消される現象が見られた．この剥離面を詳しくみると，末端の細胞

の底面に，α3（V）鎖を含む細線維のコラーゲンがびっしり付着し，その側には基底膜が形成されつつあること，その反対側の細胞面には絨毛状の突起が出現し，全くコラーゲン線維のない領域が成されているなどの，細胞に表裏の極性が生じている所見が観察された（**図5上左**Ⓐ**Ⓑ**）．またα3（V）鎖の産生は筋膜（特に浅筋膜・上筋膜）細胞に特異的であり，筋より深部に及んだ創傷ではα3（V）鎖が減少し，その領域ではコラーゲンの束が早くまとまり，線維化がより早く進行する事（**図5上右**）と，癒着が起こりやすくなる事が観察された．

これを受け，α3（V）鎖が癒着を防止するメカニズムを分子レベルで解析するため，α3（V）鎖の特異的抗体を作製し，免疫電子顕微鏡解析を用いてコラーゲン線維上での分子局在を観察した．その結果，本分子はコラーゲン線維の束に取り込まれておらず，周囲にまとわり付く付着物様の物質中に存在している事が明らかとなった（**図5下左**）．この物質はα3（V）鎖のみでなく，周囲のECM成分を巻き込んでいると考えられたため，親和性が確認されているヘパラン硫酸糖鎖特異的抗体を併用した免疫二重電顕で解析したところ，分子レベルにおいてα3（V）とヘパラン硫酸糖鎖が共局在していることが示された（**図5下左**）．これらの観察結果から，V型コラーゲンはコラーゲンが線維として会合集束する際，線維束の外周に位置して線維を整形し，径を調整するとみられているが，α3（V）鎖が加わると，ヘパラン硫酸糖鎖を含む周囲のECM分子と強くインタラクションすることにより，集束の過程が阻害され，過度の線維化を抑制するものと考えられる（**図6**）．また，α3（V）鎖を含む細線維のコラーゲンマトリックスはヘパラン硫酸糖鎖を細胞接着レセプターとして有する細胞にちょうど良い足場を提供し，またそれが接着面特異的なサイトカインのシグナルを中継点となりうることで，細胞に極性の情報を与えるものと考察できる．

つまりα3（V）鎖は①コラーゲン線維の集束形成を抑制する（抗線維化効果），②細胞に足場を提供し極性を与える（細胞の生育環境・組織の構築）という大変有用な機能を有している．さらに，α3（V）鎖は微量成分にすぎないにも拘わらず線維の形態と機能に変化を与え，コラーゲン自らによる線維化のコントロール，組織再構築を行なう実働分子として，その応用が大変期待される．

5．おわりに

肝硬変などの臓器線維症の病態はコラーゲンの無秩序な増生と蓄積であり，その治療法の戦略としてコラーゲンの合成と分解の要所が標的とされてきた．コラーゲンの合成抑制では，TGFβ，INFγ，TNFα，HGF等，コラーゲンの転写の促進・抑制にはたらく液性因子のシグナル伝達経路への遮断・介入が，広く取り組まれ，またコラーゲン遺伝子プロモーター領域・転写

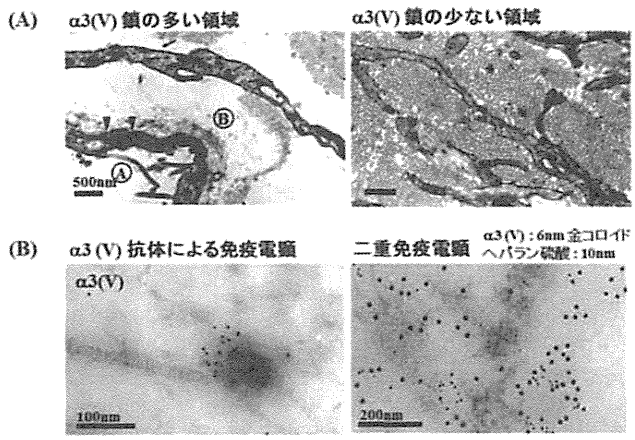

図5　V型コラーゲンα3鎖が線維構築に与える効果

（A）V型コラーゲンα3鎖の多い組織（筋膜直上）と少ない組織（筋より深部）の電子顕微鏡像．α3（V）鎖が多い組織はコラーゲンが細く保たれ，隙間が大きい．最外部の細胞はコラーゲンと接する側Ⓑに基底膜様の構造が形成され（矢頭），反対側Ⓐにはコラーゲンは全く見られず，絨毛状の突起が形成されるなどの形態変化がみられる．Barは500nm．
（B）：左α3（V）特異的抗体による免疫電子顕微鏡解析，α3（V）の局在を示す6nmの金コロイド粒子はコラーゲン線維束の外側にある不定形の付着物質の中にみられる．Barは100nm．右α3（V）抗体（6nm）とヘパラン硫酸糖鎖抗体（10nm）による二重免疫電子顕微鏡解析，両分子は線維束周囲の付着物質に共局在している．Barは200nm．
（住吉秀明，稲垣豊：医学のあゆみ Vol. 244, No 6，医歯薬出版株式会社，2013より出典）

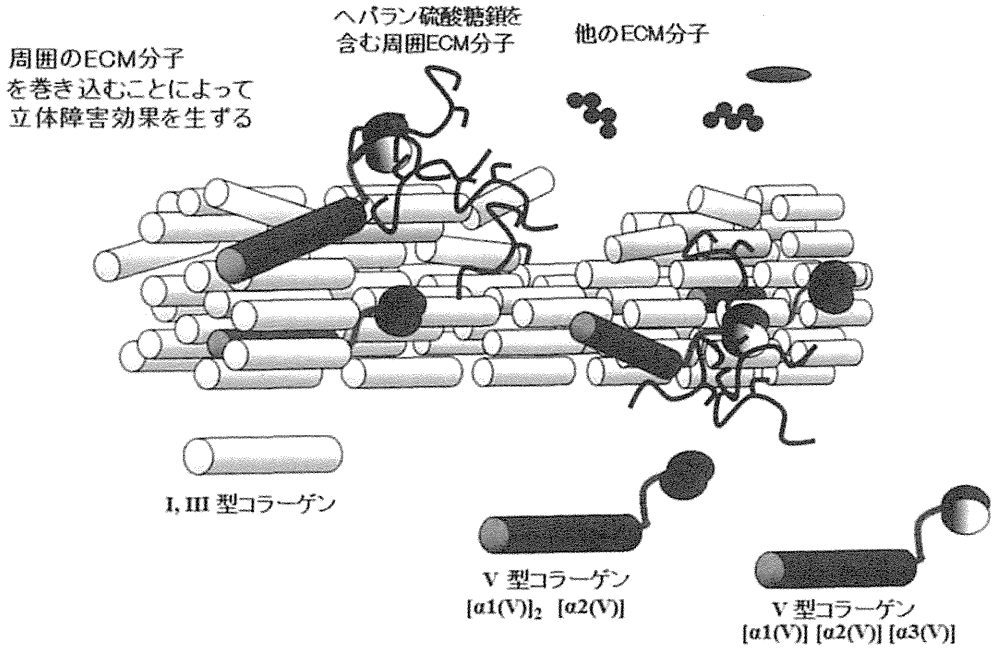

図6　α3（V）を含むV型コラーゲンが線維形成を抑制する仕組み（仮定）
（Lynsenmayer, T. F. et al. J. Cell Biol 1993.（文献2）より改変）

因子群の解析が進められた結果，特異的転写の促進・抑制シグナルに介入し，転写を抑制しうる分子標的薬の開発等の成果に結びついている[8,9]．コラーゲン分解促進においては，線維化した肝臓にコラーゲンを特異的に分解するmatrix metalloproteinases（MMPs）を導入する方法として，骨髄由来細胞を利用する方法が良好な成果を収めている[10,11]．治療への応用の為に，作用機序の異なる方法を組み合わせて用いれば，より効果的であると思われるが，コラーゲンの会合集束過程もまた，有効な線維化抑制ステップになると期待している．コラーゲンは必ずしも結晶が成長するように形成されるわけではなく，生体にはコラーゲンが絶えず生産されているにも関わらず，線維が蓄積させない仕組みがあり，それは自然で理想的な線維化の制御となりうる．その分子的な機序については，まだ手付かずの状態にあるが今回見出されたα3（V）鎖の事例は，その取り掛かりの糸口として期待される．

参考文献

1）van der Rest, M. et al.：Collagen family of proteins. FASEB J., 5：2814-2823, 1991.
2）Lynsenmayer, T. F. et al.：TypeV collagen：molecular structure and fibrillar organization of the chick-α1 (V) NH2-terminal domain, a putative regulator of corneal fibrillogenesis. J. Cell Biol., 121：1181-1189, 1993.
3）Wenstrup, J. R. et al.：Type V collagen controls the initiation of collagen fibril assembly. J. Biol. Chem., 279：53331-53337, 2004.
4）Sumiyoshi, H. et al.：Trangsient expression of mouse pro-α3 (V) collagen gene (col5a3) in wound healing. Connect. Tissue Res., 53：313-317, 2012.
5）Imamura, Y. et al.：The Pro-α3 (V) collagen chain. J. Biol. Chem., 275：8749-8759, 2000.
6）Yamaguchi, K. et al.：Pro-α3 (V) collagen chain is expressed in bone and its basic N-terminal peptide adheres to osteosarcoma cells. Matrix Biology, 24：283-294, 2005.
7）Niyibizi, C. et al.：Human placenta Type V collagens. J. Biol. Chem., 259：14170-14174. 1984.
8）Inagaki, Y. et al：Emerging insights into transforming growth factor-β Smad signal in hepatic fibrogenesis. Gut, 56：284-292. 2007
9）Higashi, K. et al.：Interferon-γ interferes with transforming growth factor-β signaling through direct interaction of YB-1 with Smad3. J Biol. Chem., 278：43470-43479 2003.
10）Sakaida, I. et al.：Transplantation of bone marrow cells reduces CCl_4-induced liver fibrosis in mice. Hepatology, 40：1304-1311. 2004.
11）Higashiyama, R. et al.：Bone marrow-derived cells express matrix metalloproteinases and contribute to regression of river fibrosis in mice. Hepatology, 45：213-222, 2007.

European Journal of Immunology

Adipose tissue derived stromal stem cell therapy in murine ConA-derived hepatitis is dependent on myeloid-lineage and CD4$^+$ T-cell suppression

Mami Higashimoto[*1], *Yoshio Sakai*[*2,3], *Masayuki Takamura*[1], *Soichiro Usui*[1], *Alessandro Nasti*[1], *Keiko Yoshida*[1], *Akihiro Seki*[1], *Takuya Komura*[1], *Masao Honda*[3], *Takashi Wada*[2], *Kengo Furuichi*[4], *Takahiro Ochiya*[5] *and Shuichi Kaneko*[1,3]

[1] Disease Control and Homeostasis, Kanazawa University, Kanazawa, Japan
[2] Department of Laboratory Medicine, Kanazawa University, Kanazawa, Japan
[3] Department of Gastroenterology, Kanazawa University Hospital, Kanazawa, Japan
[4] Division of Blood Purification, Kanazawa University Hospital, Kanazawa, Japan
[5] Division of Molecular and Cellular Medicine, National Cancer Center Research Institute, Tokyo, Japan

Mesenchymal stromal stem cells (MSCs) are an attractive therapeutic model for regenerative medicine due to their pluripotency. MSCs are used as a treatment for several inflammatory diseases, including hepatitis. However, the detailed immunopathological impact of MSC treatment on liver disease, particularly for adipose tissue derived stromal stem cells (ADSCs), has not been described. Here, we investigated the immunomodulatory effect of ADSCs on hepatitis using an acute ConA C57BL/6 murine hepatitis model. i.v. administration of ADSCs simultaneously or 3 h post injection prevented and treated ConA-induced hepatitis. Immunohistochemical analysis revealed higher numbers of CD11b$^+$, Gr-1$^+$, and F4/80$^+$ cells in the liver of ConA-induced hepatitis mice was ameliorated after the administration of ADSCs. Hepatic expression of genes affected by ADSC administration indicated tissue regeneration-related biological processes, affecting myeloid-lineage immune-mediating Gr-1$^+$ and CD11b$^+$ cells. Pathway analysis of the genes expressed in ADSC-treated hepatic inflammatory cells revealed the possible involvement of T cells and macrophages. TNF-α and IFN-γ expression was downregulated in hepatic CD4$^+$ T cells isolated from hepatitis livers co-cultured with ADSCs. Thus, the immunosuppressive effect of ADSCs in a C57BL/6 murine ConA hepatitis model was dependent primarily on the suppression of myeloid-lineage cells and, in part, of CD4$^+$ T cells.

Keywords: Adipose tissue derived stromal stem cells · Anti-inflammatory effects · CD4$^+$ T cells · ConA hepatitis · Myeloid-lineage cells

Additional supporting information may be found in the online version of this article at the publisher's web-site

Correspondence: Dr. Shuichi Kaneko
e-mail: skaneko@m-kanazwa.jp

*These authors contributed equally to this work.

Introduction

Mesenchymal stromal stem cells (MSCs) are somatic cells that reside in the mesenchymal tissues, such as the BM, umbilical cord, and adipose tissue [1,2]. MSCs are able to differentiate into several types of cells (pluripotent) in the same lineage, such as chondrocytes, osteocytes, adipocytes, and cardiomyocytes, as well as those of different lineages, such as hepatocytes. Because of this differentiation capability, they have been studied as a possible application in regenerative therapy of miscellaneous impaired organs, such as breast reconstruction [3] and repair of ischemic heart tissue [4]. Another intriguing characteristic of MSCs is their immunomodulatory potency [5]. Because most liver diseases, including viral hepatitis [6,7], primary biliary cirrhosis [8], autoimmune hepatitis [9], and steatohepatitis [10], are associated with hepatic inflammatory cells [11], elucidation of the effect of MSCs on hepatic inflammation is important when considering the use of MSCs for treating liver diseases. Although the efficacy of MSC treatment of liver diseases has been reported [12], the detailed immunopathological impact of MSC treatment on liver diseases, particularly for adipose tissue derived stromal stem cells (ADSCs), has not been investigated.

ConA, a plant lectin [13], is frequently used to induce acute hepatitis in rodents [14] to model the pathological features of autoimmune hepatitis. Although this model is mediated mainly by lymphocyte-lineage cells such as T cells and NKT cells, Kupffer cells/macrophages also participate in hepatitis. Therefore, evaluating the therapeutic efficacy of ADSCs in this murine hepatitis model is important. Although the potential efficacy of ADSCs in a BALB/c ConA hepatitis model has been reported [15], the immunopathology has not been investigated.

We confirmed that immediate i.v. administration of ADSCs after ConA injection prevented hepatitis. We also observed that administering ADSCs 3 h after the ConA injection resulted in successful treatment of hepatitis, as the liver was already infiltrated by $CD11b^+$ and $Gr\text{-}1^+$ inflammatory cells. Gene expression analysis of the liver showed that ADSC treatment affected myeloid-lineage cells, providing repair and regenerative effects in ConA-induced hepatitis mice. Moreover, gene expression analysis of hepatic inflammatory cells indicated pathways related to T cells and monocyte-lineage cells. Pathologically important cytokines such as TNF-α and IFN-γ were upregulated in $CD4^+$ T cells isolated from ConA-induced hepatitis mice but were significantly suppressed by co-culture with ADSCs. Thus, the anti-inflammatory effects of ADSCs in the C57BL/6 murine ConA hepatitis model were mediated by the suppression of myeloid-lineage and $CD4^+$ T cells.

Results

Characteristics of the immune response in ConA-induced hepatitis mice

To examine the characteristics of ConA-induced acute hepatitis, we injected 300 μg ConA into C57BL/6 female mice ($n = 4$) and determined serum alanine transferase (ALT) and lactate dehydrogenase (LDH) activities. Serum ALT and LDH activities were elevated through 24 h (Fig. 1A). The macroscopic appearance and histology of the liver obtained 24 h after ConA injection revealed intense necrosis (Fig. 1B). The immunohistochemical analysis showed that the number of $CD4^+$ T cells in the liver peaked at 6 h after the ConA injection, and remained high for 24 h (Fig. 1C and D). The numbers of $CD11b^+$ cells and $Gr\text{-}1^+$ cells accumulated in the liver increased at 3 h and reached a maximum at 12 h after ConA injection (Fig. 1C and D). The numbers of $F4/80^+$ monocyte/macrophage lineage cells increased at 6 h after the ConA injection, but returned to basal levels after 24 h (Fig. 1C and D). We also assessed the frequency of $CD11b^+/Gr\text{-}1^+$ cells, as a phenotype of myeloid-derived suppressor cells (MDSCs), in ConA hepatitis mice at 6 h ($n = 3$). The frequency of $CD11b^+/Gr\text{-}1^+$ cells was higher than that in WT mice (Fig. 1E). Scavenger receptor CD204 expression was higher in $CD11b^+/Gr\text{-}1^+$ cells than $CD11b^+/Gr\text{-}1^-$ cells (Fig. 1F), and the population gated for $CD11b^+$ cells contained granulocytic $Ly\text{-}6C^+/Ly\text{-}6G^+$ cells as well as monocytic $Ly\text{-}6C^+/Ly\text{-}6G^-$ cells (Fig. 1G).

To determine the type of immune-mediating cells involved in ConA-induced acute hepatitis, we depleted mice of various immune cell subpopulations ($n = 4$ per group). Mice that were pretreated with clodronate, a reagent that depletes monocyte-macrophage lineage cells [16], followed by injection of ConA, did not show a significant elevation in serum ALT or LDH activity (Fig. 1H). Mild elevation of serum activity for these enzymes in mice depleted of $CD4^+$ T cells was observed, whereas depletion of $CD8^+$ T cells had no significant effect. These results suggest the importance of monocyte-macrophage myeloid-lineage cells, as well as the contribution of $CD4^+$ T cells, in ConA-induced hepatitis.

ConA-induced acute hepatitis is ameliorated by i.v. administration of ADSCs in vivo

Next, we determined the therapeutic efficacy of ADSCs in the ConA-induced hepatitis model. We obtained and expanded stromal cells from adipose tissue by passaging them eight to ten times (Fig. 2A). Almost all cells expressed the mesenchymal lineage markers, CD29 and CD44 (Fig. 2B). With regard to stem cell markers [17], approximately 40% and 73% of cells expressed CD105 and CD90, respectively (Fig. 2B). Moreover, the cells were pluripotent and were able to differentiate into osteocytes, chondrocytes, and adipocytes (Fig. 2C–F). When 1×10^5 ADSCs were administered via the tail vein immediately after ConA injection in mice ($n = 3$), the elevation of serum ALT and LDH activity was substantially ameliorated, compared with mice without ADSC treatment ($n = 4$) 24 h after injection (Fig. 3A). In terms of therapeutic efficacy, 1×10^5 ADSCs were administered to mice 3 h after ConA injection ($n = 3$), serum ALT and LDH activities were significantly reduced in acute hepatitis mice treated with ADSCs, compared with ConA-induced hepatitis mice without treatment ($n = 4$), 24 h after ConA administration (Fig. 3B). The macroscopic

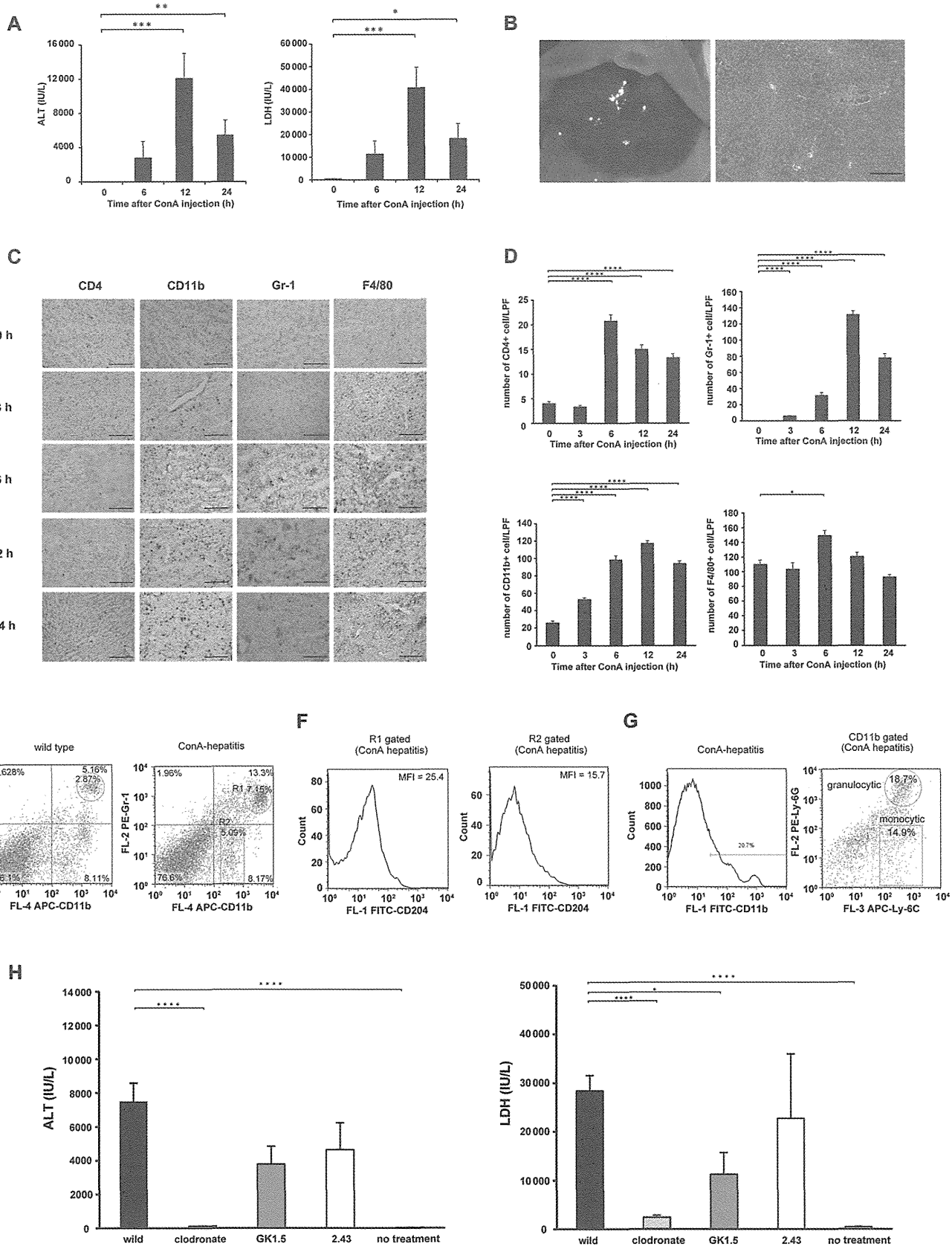

appearance of the liver obtained from mice injected with 300 μg of ConA followed by ADSC administration showed a mild and spotty white area with an almost normal color (Fig. 3C). Liver histology showed an almost normal appearance, with no necrosis (Fig. 3C), indicating that ConA-induced hepatitis was markedly ameliorated by ADSC treatment. No preventive or therapeutic effect on ConA-induced hepatitis resulted from administration of primary cultured murine hepatocytes ($n = 3$); there was no significant reduction in serum ALT or LDH (Fig. 3A and B), macroscopic necrosis appearance, or histological necrosis, compared with ConA-induced hepatitis (Fig. 3C).

ADSC treatment reduces elevated cytokine/chemokine concentrations in ConA-induced hepatitis mice

Marked protective and therapeutic effects of ADSCs on ConA-induced hepatitis were observed. To determine the effect of ADSC treatment on systemic inflammation in ConA-induced hepatitis, we measured serum cytokine and chemokine concentrations in ConA-induced hepatitis mice treated with ADSCs. Mice injected with ConA were immediately treated with ADSCs and serum was collected 6 h after ConA injection ($n = 3$). The elevated serum IFN-γ, IL-2, IL-6, IL-4, IP-10, MIG, KC, and MCP-1 levels in ConA-injected mice ($n = 3$) were significantly reduced by ADSC treatment (Supporting Information Fig. 1A). Injection of mice with ADSCs 3 h after ConA administration ($n = 4$) resulted in significantly reduced serum IFN-γ, IL-2, IL-6, and MIG levels, compared to ConA-injected mice not treated with ADSCs ($n = 6$) (Supporting Information Fig. 1B). Thus, the levels of the array of cytokines and chemokines that are elevated in the sera of ConA-induced hepatitis mice were significantly decreased by ADSC treatment.

Distribution of i.v. administered ADSCs in ConA-induced hepatitis murine models

The distribution of administered ADSCs in ConA-induced hepatitis mice was determined by immunohistochemistry. Administered GFP-expressing ADSCs were observed in the lung, but not the liver, of mice injected with ConA followed by immediate ADSC administration ($n = 6$), through 24 h (Supporting Information Fig. 2A). When administered to mice 3 h after ConA injection ($n = 6$), GFP-expressing ADSCs were observed primarily in the lung, and a few in the liver (Supporting Information Fig. 2B), suggesting that some fraction of ADSCs reached the liver upon occurrence of hepatitis.

Hepatic gene expression changes by ADSCs treatment are associated with Gr-1$^+$ and CD11b$^+$ cells

To investigate the detailed biological features of the liver in ConA-induced hepatitis mice that were treated with ADSCs, we examined the gene expression profiles of liver tissue of ConA-injected mice obtained 2 h after treatment with ADSCs using a DNA microarray. In the liver tissues of mice treated with ADSCs immediately after ConA injection ($n = 3$), 589 gene probes were differentially expressed compared with that in mice with ConA-induced hepatitis that had not been treated with ADSCs ($n = 3$). Expression of the majority of genes was downregulated by ADSCs, as shown by green color ($p < 0.05$; Fig. 4A). Principal component analysis using these genes showed a discernible distribution difference between the ADSC-treated and -untreated groups (Fig. 4B). When mice received ADSC treatment 3 h after ConA injection, hepatic expression of 309 gene probes was altered significantly compared with those in mice with ConA-induced hepatitis that had not been treated with ADSCs ($n = 3$). Expression of the majority of genes was downregulated by ADSCs, as shown by green color ($p < 0.01$; Fig. 4C). Principal component analysis of these genes also showed a discernible distribution difference between the ADSC-treated and untreated groups (Fig. 4D). In the context of biological maps of the genes affected by immediate ADSC treatment, cell differentiation, the inflammatory response, the DNA damage response, and apoptosis predominated (Supporting Information Table 1). In addition to these maps, tissue remodeling and wound repair, mitogenic signaling, and vascular development (angiogenesis) predominated in mice that had received ADSC treatment 3 h after ConA injection (Table 1), indicating that ADSCs provided not only anti-inflammatory effects, but also remodeling effects, in the ConA-damaged liver.

◀ **Figure 1.** Characteristics of ConA-induced hepatitis in C57BL/6 mice. (A–D) C57BL/6 female mice were injected i.v. with 300 μg of ConA. Sera and liver tissues were obtained 3, 6, 12, and 24 h after ConA injection. The data are representative of three individual experiments. (A) ALT and LDH activity in sera. Results are expressed as means ± SE ($n = 4$). $^*p < 0.05$, $^{**}p < 0.01$, $^{***}p < 0.005$ versus 0 h (Student's *t*-test). (B) Representative liver tissues obtained 12 h after ConA injection were assessed macroscopically and microscopically. Magnification: ×100. Bar: 200 μm. (C) Immunohistochemical staining for CD4, CD11b, Gr-1, and F4/80 in the livers of mice for each time point (0, 3, 6, 12, and 24 h; $n = 4$ per time point). Representative images of mice for each time point are shown. Magnification: ×100. Bar: 200 μm. (D) Quantification of the number of CD4$^+$, CD11b$^+$, Gr-1$^+$, and F4/80$^+$ cells in four visual fields per ×100 low-power field in the livers of representative mice in each group. Magnification: ×100. $^*p < 0.05$, $^{****}p < 0.001$ versus untreated mice (Student's *t*-test). (E–G) Hepatic inflammatory cells were isolated from mice 6 h after ConA injection, incubated with fluorescence-conjugated antibodies, and assessed by FACS. Three mice per group per experiment. Experiments were performed twice. (E) Frequency of CD11b$^+$Gr-1$^+$ cells in WT C57BL/6 mice and ConA hepatitis mice. (F) Analysis of CD204 expression in CD11b$^+$Gr-1$^+$ cells (R1-gated region in (E)) and CD11b$^+$Gr-1$^-$ cells (R2-gated region in (E)) among hepatic inflammatory cells from ConA hepatitis mice. MFI: mean fluorescence intensity. (G) CD11b$^+$ cells among hepatic inflammatory cells from ConA hepatitis mouse were gated, and Ly-6C and Ly-6G expression levels in the gated cells were determined. (H) C57BL/6 female mice were injected i.v. with clodronate ($n = 4$), i.p. with anti-CD4 antibody (GK1.5) ($n = 4$), or anti-CD8 antibody (2.43) ($n = 4$) every 24 h for 2 days. The mice were then injected i.v. with 300 μg of ConA. Sera were obtained 24 h after ConA injection, and ALT and LDH activities were then measured. Results are expressed as means +SE ($n = 4$ per group) and are representative of one experiment performed. $^*p < 0.05$, $^{****}p < 0.001$ versus ConA-injected WT mice ($n = 4$) (Student's *t*-test).

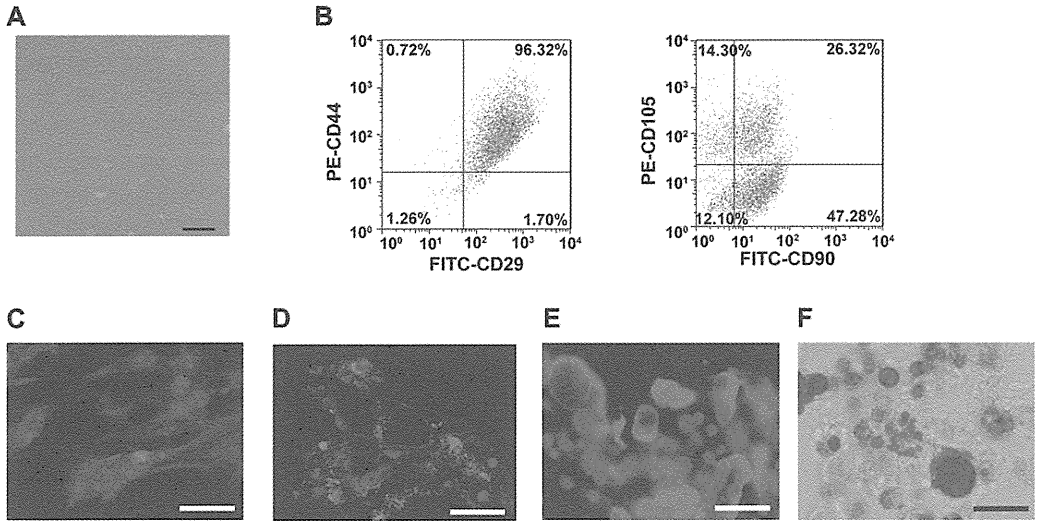

Figure 2. Characteristics and pluripotency of cultured ADSCs. Cells in the stromal fraction of adipose tissues from mice were cultured, maintained, and expanded for eight to ten passages. (A) Spindle shaped cells were observed after eight passages. Magnification: ×100. Bar: 200 μm. (B) Flow cytometric analysis of CD29, CD44, CD90, and CD105 surface marker expression. The data shown are representative of three independent experiments. (C–F) ADSCs were cultured with specific growth factors for induction of osteocytes, chondrocytes, and adipocytes using a mouse mesenchymal stem cell functional kit. Immunohistochemical staining was performed with (C) anti-osteopontin antibody for osteocytes, (D) anti-collagen II antibody for chondrocytes, and (E) anti-FABP antibody as well as (F) Oil-Red O staining for adipocytes. Magnification: x200. Bars: 50 μm. All data shown are from one experiment representative of two independent experiments performed.

Next, we investigated the relevance of these altered genes in the context of inflammatory cells using the public gene expression database of hematopoietic cells and stem cells (GSE27787). The annotated genes among the 589 gene probes detected by microarray analysis probes in the livers of mice that received ADSC treatment immediately after ConA injection were not relevant to any hematopoietic cell type (Fig. 4E). By contrast, among the 309 gene probes, the majority of the annotated genes whose hepatic expression in mice that received ADSC treatment 3 h after ConA injection was affected significantly were found to be highly expressed in Gr-1$^+$ cells and Mac1$^+$ (CD11b$^+$) cells — as indicated by the red color (Fig. 4F). Since majority of the 309 gene probes in the liver of ConA hepatitis were downregulated by ADSC treatment, as indicated by green color (Fig. 4C), these results suggested that effects on Gr-1$^+$ and CD11b$^+$ cells were associated with the therapeutic effect of ADSCs 3 h after ConA injection.

ADSC treatment represses inflammatory cell accumulation in ConA-induced hepatitis

To determine the influence of ADSC treatment on the infiltration/accumulation of immune-mediating cells in the liver of ConA-induced hepatitis mice, we assessed by immunohistochemistry the inflammatory cells in the liver tissues of mice injected with ConA followed by ADSC administration at 3 h. Liver tissues obtained at 6, 12, and 24 h ($n = 4$ each time point) after ConA injection showed reduced accumulation of CD11b$^+$ cells, Gr-1$^+$ cells, and F4/80$^+$ cells after ADSC treatment (Fig. 5). In contrast, the increased number of infiltrated CD4$^+$ T cells in ConA-induced hepatitis mice was not significantly affected by the ADSCs (Fig. 5). Thus, the predominant change in ConA-induced hepatitis mice treated with ADSCs was in the number of myeloid-lineage inflammatory cells, consistent with the hepatic gene expression data.

T-cell involvement in the altered gene expression of hepatic inflammatory cells by ADSCs treatment

To further assess the anti-inflammatory effects of ADSCs in mice with ConA-induced hepatitis, we isolated hepatic inflammatory cells from mice 2 h after ADSC treatment, which was administered 3 h after ConA injection ($n = 2$) and from mice not treated with ADSCs ($n = 2$). A total of 939 genes were differentially expressed in hepatic inflammatory cells from ConA-induced hepatitis mice treated with ADSCs. The gene expression profiles associated with ADSC treatment and ConA-induced hepatitis without ADSC treatment were readily distinguishable (Supporting Information Fig. 3A). Pathway map analysis showed that these genes were relevant to biological pathways of oncostatin M signaling via JAK-Stat or MAPK signaling and CCR5 signaling in macrophages and T lymphocytes in the immune response pathway (Supporting Information Table 2). Network analysis of these genes featured a network consisting of AcRIIA, STAT3, Activin A, FTSJD1, and STAT1 at the top (Supporting Information Table 3), which indicated that pathways involving IL-2 and TNF-α, and the STAT1/STAT3 pathway were also involved (Supporting Information Fig. 3B). These results suggest that T cells, as well as antigen presenting/phagocytosis lineages, were the immune-mediating cell populations affected by ADSC treatment.

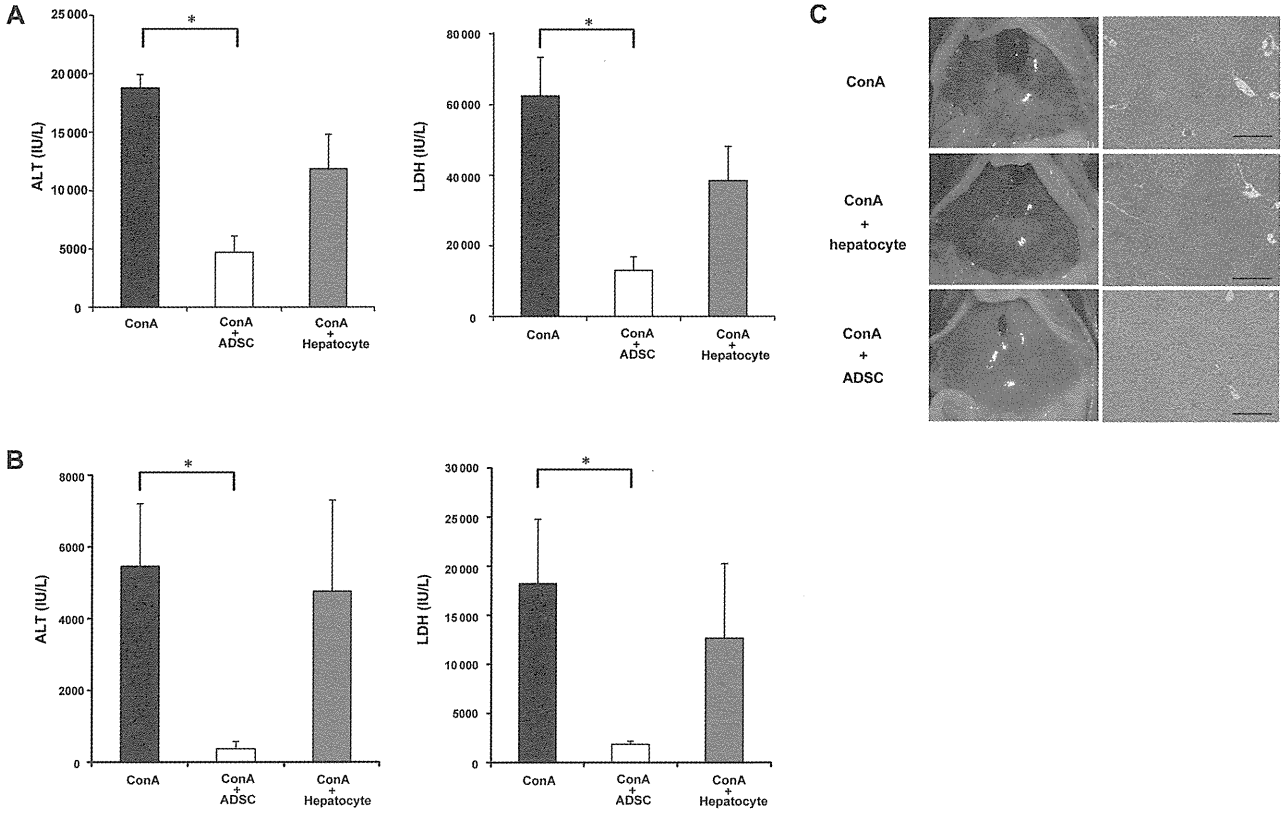

Figure 3. Therapeutic effects of ADSCs in ConA-induced hepatitis. C57BL/6 female mice were injected i.v. with 300 μg of ConA. Immediately or 3 h later, 1×10^5 ADSCs or hepatocytes were injected via the tail vein. Liver tissues and blood samples were obtained 24 h after ConA injection. Liver tissues were examined histologically and serum ALT and LDH activities were measured. (A, B) Serum ALT and LDH activities of mice injected with ConA followed by ADSC injection (A) immediately or (B) 3 h later. ConA: ConA-injected mice without treatment ($n = 4$), ConA + ADSC: ConA-injected mice followed by ADSC treatment ($n = 3$), ConA + hepatocyte: ConA-injected mice followed by primary cultured hepatocyte treatment ($n = 3$). Data are shown as mean ± SE and are from one experiment representative of two independent experiments. $^*p < 0.05$ (Wilcoxon signed-rank test), compared with ConA-injected mice. (C) Macroscopic appearance of the liver (left) and histology of the liver tissues as assessed by H&E staining (right). Magnification of histology: ×100. Bars: 200 μm. Images shown are from one mouse representative of three to four mice from each group studied.

ConA-activated CD4$^+$T cells and CD11b$^+$ cells in the liver are important targets of ADSC treatment

The above data indicated that ADSCs administered in ConA-induced hepatitis had therapeutic immunological effects in terms of repairing the damaged liver and affected CD11b$^+$ and Gr-1$^+$ myeloid-lineage cells and T cells. To further explore how ADSCs affected the subpopulations of inflammatory cells involved in ConA-induced hepatitis, we investigated the expression of cytokine/chemokine-related genes in CD4$^+$ T cells and CD11b$^+$ cells obtained from livers with ConA-induced hepatitis ($n = 4$) that had been treated in vitro with ADSCs ($n = 3$). Expression of TNF-α, IL-10, and CXCL10 was significantly downregulated by ADSC treatment in both CD4$^+$ T cells (Supporting Information Fig. 4A) and CD11b$^+$ cells (Supporting Information Fig. 4B). IFN-γ, IL-4, and CXCL9 expression by CD4$^+$ T cells were significantly affected by ADSCs. Although CCL3, which was upregulated by ConA injection, was not significantly affected by ADSCs, the expression of its cognate receptor, CCR5, was decreased in CD4$^+$ T cells (Supporting Information Fig. 4A), suggesting an effect on the CCL3-CCR5 axis. These results suggest that CD4$^+$ T cells and myeloid-lineage CD11b$^+$ cells were the susceptible hepatic inflammatory subpopulations of cells in the ConA-induced hepatitis liver.

Anti-inflammatory effect of ADSCs on ConA hepatitis do not rely on MDSCs

We further assessed whether the anti-inflammatory effect of ADSCs in ConA hepatitis relied on MDSCs. Neither the frequency of nor the NO production by CD11b$^+$Gr-1$^+$ cells were increased by ADSC treatment (Supporting Information Fig. 5A). CD11b$^+$Gr-1$^+$ cells from ConA-injected mice treated with ADSCs showed arginase activity similar to that in CD11b$^+$Gr-1$^+$ cells from ConA-injected mice (Supporting Information Fig. 5B). CD11b$^+$Gr-1$^+$ cells from ConA-injected mice treated with ADSCs suppressed the ConA-stimulated proliferation of T cells in vitro, although the effect was slightly attenuated compared to that of cells from mice with ConA-induced hepatitis (Supporting Information Fig. 5C). Thus, ADSC treatment was not dependent on MDSCs induced by ConA hepatitis.

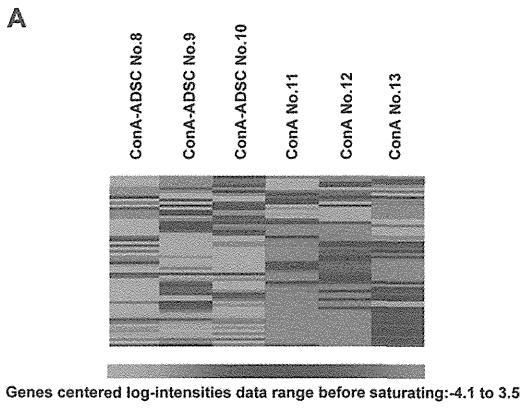

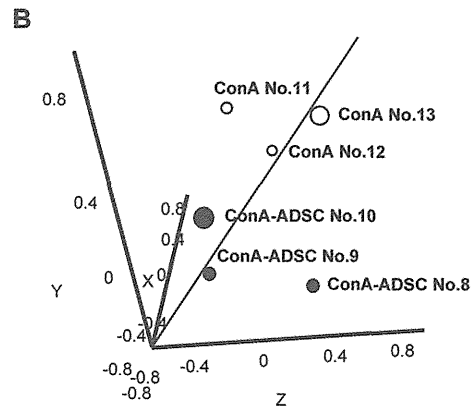

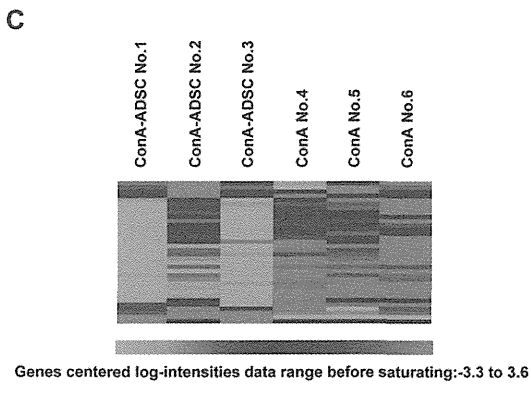

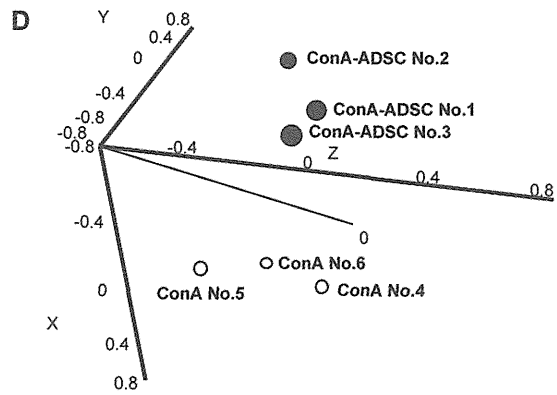

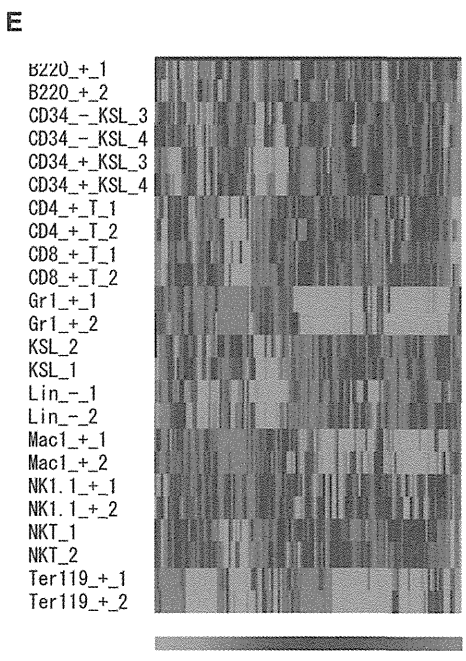

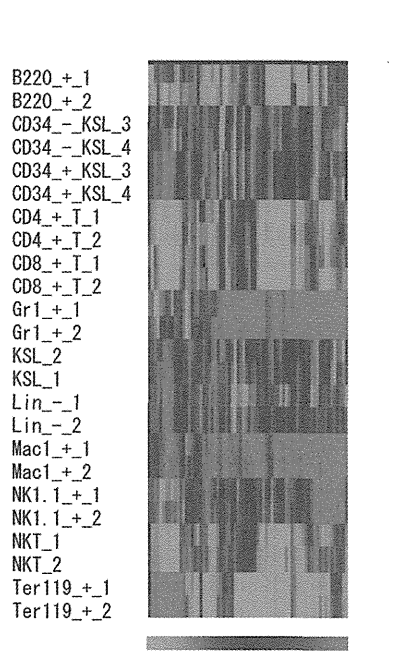

Discussion

MSCs are effective for immune-mediated disease treatment including the ConA-induced BALB/c murine hepatitis model [15], but the detailed mechanisms have not been fully elucidated. Here, we confirmed that ADSCs have preventive and therapeutic effects in a ConA-induced C57BL/6 hepatitis murine model and assessed the immunopathological mechanisms by determining the participating hepatic immunomodulatory cells. ADSCs injected via the tail vein were found in the lung; some were observed in the liver but only when ADSCs were administered 3 h after ConA injection, a time at which infiltration of $CD11b^+$ and $Gr\text{-}1^+$ inflammatory cells into the liver had already begun. Gene expression analysis of liver tissue from ConA-induced hepatitis mice showed that the ADSC treatment induced biological pathways indicative of liver repair and regeneration. Myeloid-lineage cells were the predominant population in terms of affected genes, consistent with immunohistochemical staining of the liver for immune-mediating cells. Furthermore, the gene expression profiles of hepatic inflammatory cells from ConA-induced hepatitis mice treated with ADSCs suggested T-cell and macrophage involvement. Moreover, the expression patterns of cytokine/chemokine-related genes in hepatic inflammatory cells co-cultured with ADSCs suggested that $CD4^+$ T cells were important in ConA-induced hepatitis and were affected by ADSC treatment.

The immunopathological features of ConA-induced hepatitis have been characterized as being primarily lymphocyte-lineage cell-mediated hepatitis [18–20], leading to massive hepatocellular degeneration, necrosis, and apoptosis [21]; thus, this model is relevant to clinical autoimmune hepatitis. Additionally, Kupffer cells play an important role in induction of hepatitis [22]. Unexpectedly, we observed prominent increases in $CD11b^+$, $Gr\text{-}1^+$, and $F4/80^+$ cells in liver tissues of the ConA-induced hepatitis mice. Additionally, we found that the monocyte-macrophage lineage cells contributed most significantly to hepatitis, as confirmed by depletion treatment, such that hepatitis was almost completely abolished when those cell types were abrogated by clodronate. This is further evidenced by the fact that ADSC treatment reduced the number of $CD11b^+$, $Gr\text{-}1^+$, and $F4/80^+$ cells in the liver of ConA-induced hepatitis mice (Fig. 5). The importance of $Gr\text{-}1^+$ and $CD11b^+$ cells was also suggested by changes in the gene expression profile of the liver of ConA-induced hepatitis treated with ADSCs (Fig. 4C and F). Thus, monocyte-macrophage lineage cells are important in the pathogenesis of ConA-induced hepatitis in mice and are important targets of ADSCs. $CD4^+$ T cells were also involved since their depletion partially ameliorated ConA-induced hepatitis. The number of infiltrating $CD4^+$ T cells in the liver of ConA-induced hepatitis mice was not markedly reduced by ADSC treatment. However, gene expression analysis of hepatic inflammatory cells in ConA-induced hepatitis mice treated with ADSCs showed that signaling of oncostatin M, a type I cytokine associated with developing T cells [23], and CCR5 signaling in macrophages and T lymphocytes were affected. Therefore, $CD4^+$ T cells participate as an immune mediator and therapeutic target of ADSCs in the pathology of ConA-induced hepatitis mice.

With regard to cytokine/chemokine-related gene expression in hepatic inflammatory cells of ConA-induced hepatitis mice, expression of TNF-α, IL-10, and CXCL10 in $CD4^+$ T cells and $CD11b^+$ cells was downregulated by ADSC treatment (Supporting Information Fig. 4). Additionally, IFN-γ, IL-4, and CXCL9 were also significantly downregulated in $CD4^+$ T cells, but not in $CD11b^+$ cells (Supporting Information Fig. 4). Changes in the expression of the Th2 cytokines, IL-10 and IL-4, were considered to be the secondary consequence of ConA-induced hepatitis, mediated by TNF-α and/or IFN-γ, which are characterized as Th1-associated cytokines [24]. CCR5 expression by $CD4^+$ T cells was downregulated by ADSCs, which may be relevant to the biological processes indicated by the downregulated genes in hepatic inflammatory cells. Because CCR5 is a $CD4^+$ T-cell receptor that interacts with APCs, such as macrophages [25], suppression of CCR5 expression on $CD4^+$ T cells by ADSC might explain the amelioration of ConA-mediated hepatitis. Overall, the therapeutic efficacy of ADSCs impacted both $CD4^+$ and $CD11b^+$ cells in terms of alteration of levels of inflammatory humoral mediators and cytokine/chemokine profiles, thus contributing to amelioration of ConA-induced hepatitis.

A proportion of i.v. administered ADSCs were present in the livers of ConA mice injected with ADSCs at a time point at which the liver had already been infiltrated with $Gr\text{-}1^+$ and $CD11b^+$ cells, whereas no ADSCs were present in the livers of mice injected with ConA following immediate treatment with ADSCs. This indicates that a liver undergoing inflammation attracts administered ADSCs. The extent of inflammation required to recruit ADSCs should be clarified, as it has previously been reported that hepatitis occurring just 30 min after ConA injection results in recruitment of a substantial number of stem cells to the liver in the BALB/c ConA hepatitis model [15]. Given that the migratory capabilities of MSCs are well known although not yet fully investigated [26], how ADSCs are recruited to an already inflamed liver as a result of ConA administration should be examined. In addition, the ADSCs administered to C57BL/6 mice immediately after ConA injection resided in the lung. In spite of the fact that they were not detected in the liver, these ADSCs prevented ConA hepatitis, indicating the remote effect of ADSCs. Thus, indirect mediators produced by ADSCs associated with their anti-inflammatory effects should be investigated intensively.

◀ **Figure 4.** Gene expression analysis in the liver of ConA-induced hepatitis mice treated with ADSCs. C57BL/6 female mice were injected i.v. with 300 μg of ConA. (A, B, and E) Immediately or (C, D, and F) 3 h after ConA injection, mice were treated with 1×10^5 ADSCs via the tail vein ($n = 3$ each). Liver tissues were analyzed 2 h after ADSC administration and RNA was isolated for gene expression analysis using a DNA microarray. Data shown are from one experiment performed. (A, B) One-way clustering analysis (A) and principal component analysis (B) of the 589 differentially expressed genes in treated and untreated ConA-injected mice. (C, D) One-way clustering analysis (C) and principal component analysis (D) of the 309 differentially expressed genes in treated (after 3 h) and untreated ConA-injected mice followed. Colors indicate the intensity of gene upregulation (red), downregulation (green), and no change (black). (E, F) One-way clustering analysis of gene expression in hematopoietic and stem cells (GSE27787) for annotated genes among the 589 (E) and 309 (F) genes.

Table 1. Maps relevant to genes for which the expression was affected in the liver of ConA-injected mice followed by ADSC treatment at 3 h.

Maps	*p*-value
Tissue remodeling and wound repair	0.000001438
Inflammatory response	0.000003973
Mitogenic signaling	0.0001056
Vascular development (angiogenesis)	0.0002926
DNA damage response	0.0004529
Apoptosis	0.0008909
Cystic fibrosis disease	0.001402
Myogenesis regulation	0.001571
Cell differentiation	0.002173
Immune system response	0.003304

In conclusion, the therapeutic anti-inflammatory efficacy of ADSCs relied on suppression of myeloid-lineage and $CD4^+$ T cells in the ConA-induced C57BL/6 murine hepatitis model. The application of ADSC therapy to various inflammatory liver diseases can be further developed by studies of their immunomodulatory effects.

Materials and methods

Murine acute hepatitis induced by ConA injection and treatment with ADSCs

C57BL/6J female mice (10–12 weeks old, Charles River Laboratories Japan Inc., Yokohama, Japan) were injected i.v. with 300 μg of ConA (Sigma-Aldrich, St. Louis, MO, USA) dissolved in PBS. For $CD4^+$ T-cell or $CD8^+$ T-cell depletion, 200 μg of purified anti-CD4 antibody from the culture supernatant of GK1.5 cells (ATCC, Manassas, VA, USA), or purified anti-CD8 antibody from the culture supernatant of 2.43 cells (ATCC), was injected i.p. for two consecutive days before ConA injection. For depletion of monocyte-macrophage lineage cells, 2 mg of clodronate (Sigma-Aldrich), which was encapsulated in liposomes using the COATSOME-EL-01-N liposome formulation kit (Nihonyushi, Tokyo, Japan) [27], was injected via the tail vein 2 days before ConA injection. For the prevention or treatment experiment, 1×10^5 ADSCs were administered i.v. immediately or 3 h after ConA injection. In some cohorts, blood was obtained under anesthesia, and liver and lung tissues were collected after euthanizing mice at 6, 12, and 24 h after ConA injection. A portion of the liver tissue was homogenized and the enriched fraction of inflammatory cells was obtained by gradient centrifugation using Ficoll–Hypaque (Sigma-Aldrich). Our institutional review board approved the care and use of laboratory animals in all experiments.

Isolation and culture of ADSCs and primary hepatocytes

Inguinal adipose tissues were obtained from C57BL/6J male mice (10–12 weeks old, Charles River Laboratories Japan Inc.) or GFP-transgenic mice (male, 10–12 weeks old, gift from Prof. Okabe, Osaka University, Japan). Tissues were digested with 0.075% collagenase type I (Wako Pure Chemical Industries Ltd., Osaka, Japan), washed with PBS, and then transferred to a culture dish with DMEM/F-12 1:1 medium (Life Technologies–Invitrogen, Carlsbad, CA, USA) supplemented with 10% heat-inactivated FBS and 1% antibiotic–antimycotic solution (Life Technologies). Cells were maintained and expanded by eight to ten passages before use.

To obtain primary hepatocytes, C57BL/6J male mice (10–12 weeks old) were anesthetized by i.p. injection of pentobarbital (50 mg/kg; Kyoritsu Seiyaku, Tokyo, Japan) and injected with 10 mL of 0.75% type I collagenase solution via the portal vein. Liver tissues were minced to dissociate cells, filtered through a 100 μm mesh, and cultured in 10-cm culture dishes for 16 h until use.

Pluripotency of ADSCs

The pluripotency of ADSCs was examined using a mouse mesenchymal stem cell functional kit® (R&D Systems, Minneapolis, MN, USA), and immunohistochemical staining of cells that had differentiated into osteocytes, chondrocytes, and adipocytes was performed using anti-mouse ostepontin, anti-mouse collagen II, and anti-mouse FABP4 antibodies, respectively, in accordance with the manufacturer's instruction. Adipocyte differentiation was also assessed by staining using an aliquot of Oil Red O (WAKO).

Co-culture of ConA-stimulated hepatic inflammatory cells with ADSCs

Hepatic inflammatory cells were isolated from C57BL/6J female mice (10 weeks old) that had been injected i.v. with 300 μg of ConA 3 h before ($n = 4$). $CD4^+$ T cells and $CD11b^+$ cells were separated from the collected hepatic inflammatory cells using anti-CD4 and anti-CD11b magnetic beads (Miltenyi Biotec, Bergisch Gladbach, Germany). Then, 20 000 ADSCs were co-cultured with 4×10^5 of the isolated $CD4^+$ T cells or $CD11b^+$ cells in a 24-well plate (BD Falcon, San Jose, CA, USA) for 2 h ($n = 3$). After co-culture, floating cells were harvested, and RNA harvested using the MicroRNA isolation kit (Stratagene, La Jolla, CA, USA) for real-time PCR analysis to measure cytokine/chemokine gene expression.

Measurement of serum ALT and LDH activity

Blood was collected from the postorbital venous plexus and serum was separated from clotted blood after coagulation. The serum activity of ALT, and LDH was measured using L-type WAKO GPT J2, and LDH-J kits (Wako Pure Chemical Industries Ltd.), respectively, using autoanalytical equipment (Hitach7180, Hitachi Ltd., Tokyo, Japan), according to the manufacturer's protocol.

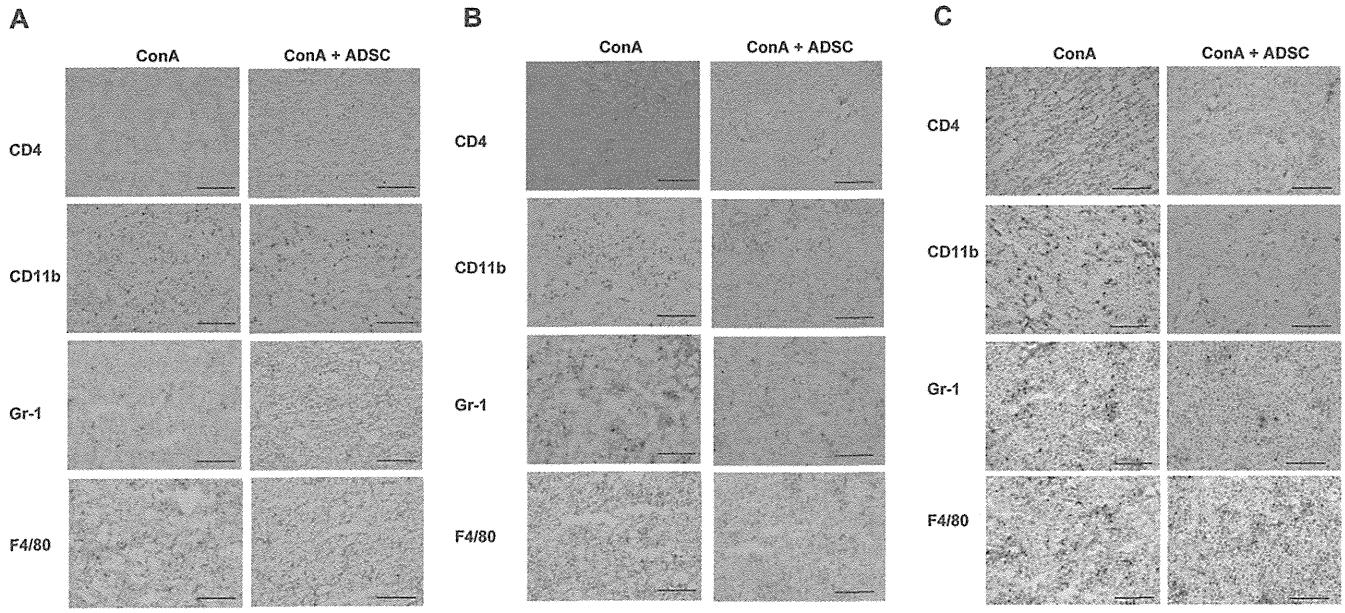

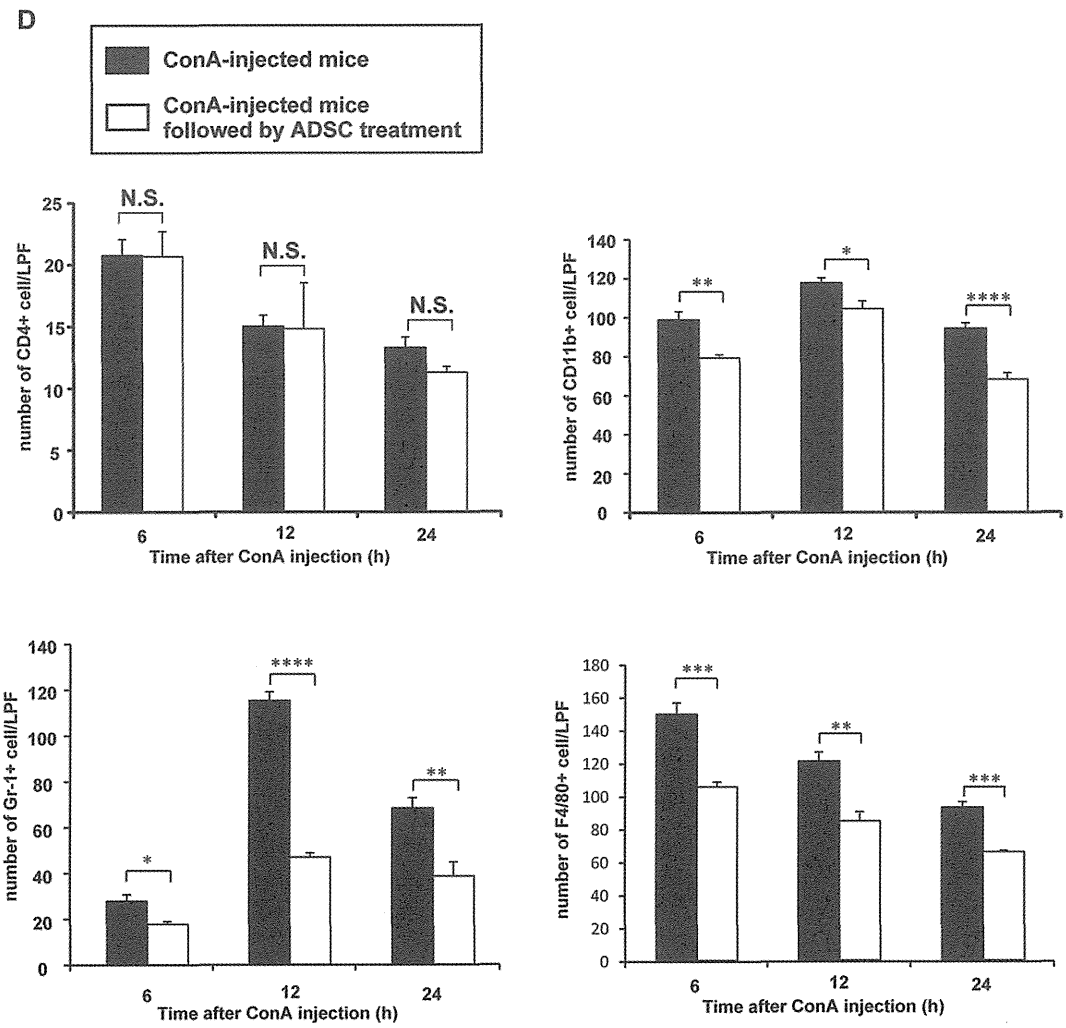

Measurement of serum cytokine/chemokine concentrations

Sera were obtained from ADSC-treated mice immediately or 3 h after ConA injection ($n = 3$ and $n = 4$, respectively), and from ConA-injected mice not treated with ADSCs ($n = 3$ and $n = 6$, respectively) at 6 h. Serum concentrations of cytokines and chemokines were measured using a Multiplex Bead Immunoassays kit, Mouse Cytokine 20-Plex Panel (Invitrogen, Carlsbad, CA, USA), following the manufacturer's protocol. The kit covers FGF-basic, GM-CSF, IFN-γ, IL-1α, IL-1β, IL-2, IL-4, IL-5, IL-6, IL-10, IL-12 (p40/p70), IL-13, IL-17, IP-10(CXCL10), KC, MCP-1, MIG(CXCL9), MIP-1α, TNF-α, and VEGF.

Histological and immunohistochemical analyses of liver and lung tissues

Harvested liver and lung tissues were fixed in 10% formaldehyde, embedded in paraffin, sectioned at 4 μm, and stained with H&E. For immunohistochemical analysis, the liver tissues were embedded in OCT compound (Sakura Finetek, Torrance, CA, USA), snap-frozen in liquid nitrogen, cryostat-sectioned, and fixed with methanol/acetone (1:1). The paraffin-embedded tissues were also sliced into 4 μm sections, mounted on microscope slides, and deparaffinized, followed by epitope retrieval using proteinase K (Dako, Glostrup, Denmark). The slides were incubated with peroxidase blocking reagent (Dako) for 15 min at room temperature to inhibit endogenous peroxidase activity, followed by incubation with protein blocking reagent (Dako) to avoid nonspecific protein reactions. The slides were incubated with primary antibodies (anti-mouse CD4, CD11b, Gr-1, F4/80) (BD Pharmingen, San Diego, CA, USA) and anti-GFP (MBL, Nagoya, Japan) diluted with PBS containing 1% BSA overnight at 4°C. After washing in PBS, the slides were then incubated with secondary antibodies (anti-rat, anti-rabbit; Nichirei, Japan) for 30 min at room temperature. The immune complexes were visualized using EnVision kits /HRP (DAB; Dako) followed by counterstaining with hematoxylin. The numbers of positive cells in each section were counted in four randomly selected fields at 100× magnification under a microscope.

RNA isolation and gene expression analysis by DNA microarray

Total RNA was obtained from the tissues or hepatic inflammatory cells in RNAlater (Ambion) using RNA isolation kit (Sigma-Aldrich) in accordance with the supplied protocol with slight modifications. Isolated RNA was amplified and labeled with the Cy3 using the Quick Amp labeling kit (Agilent Technologies, Santa Clara, CA, USA) in accordance with the manufacturer's protocol. cRNA of 1.65 μg was hybridized onto a Whole Mouse Genome 4 × 44K Array (Agilent Technologies) and scanned using a DNA Microarray Scanner (model G2505B, Agilent Technologies).

Gene expression data were analyzed using the GeneSpring analysis software (Agilent Technologies). Each measurement was divided by the 75th percentile of all measurements in that sample at per chip normalization. Hierarchical clustering and principal component analysis of gene expression was performed. Welch's *t*-test, with Benjamini and Hochberg's false discovery rate, was used to identify genes that were differentially expressed in the groups of interest. Analysis of biological processes was performed using the MetaCore software suite (GeneGo, Carlsbad, CA, USA). BRB array tools (http://linus.nci.nih.gov/BRB-ArrayTools.html) were also used for unsupervised or one-way clustering analyses. Microarray data were deposited in the NBCI Gene Expression Omnibus (GSE ID: GSE41465).

Flow cytometry

Cultured ADSCs were incubated in PBS supplemented with 2% BSA (Sigma-Aldrich) containing antibodies labeled with FITC or PE anti-mouse CD44 or CD90 (Beckman Coulter, Brea, CA, USA), and CD105 (Miltenyi Biotec) antibodies. Hepatic inflammatory cells isolated from mice were incubated with a mixture of FITC-labeled anti-mouse CD204 (AbD Serotec, Raleigh, NC, USA), PE-labeled anti-mouse Gr-1 (Miltenyi Biotec), and allophycocyanin-labeled anti-mouse CD11b (BioLegend, San Diego, CA, USA), or FITC-labeled anti-mouse CD11b (Beckman Coulter), PE-labeled anti-mouse Ly-6G (BioLegend), and allophycocyanin labeled anti-mouse Ly-6C (BioLegend) antibodies. The fluorescence intensity of the cells was measured using a FACSCalibur™ (Becton Dickinson, San Jose, CA, USA). Data obtained were visualized and analyzed using the FlowJo software (Tomy Digital Biology Co., Ltd., Tokyo, Japan).

Isolation of $CD11b^+Gr\text{-}1^+$ hepatic inflammatory cells and T-cell [3H]-thymidine incorporation assay

C57BL/6J female mice were injected with 300 μg of ConA and then injected with 1×10^5 ADSCs after 3 h ($n = 3$). Three

Figure 5. Immunohistochemical analysis of inflammatory cells in the liver of ConA-induced hepatitis mice treated with ADSCs. (A–C) Immunohistochemical staining of the liver. C57BL/6 female mice were injected i.v. with 300 μg of ConA. Then, 3 h later, the mice were injected with ADSCs via the tail vein. Liver tissues were obtained at (A) 6, (B)12, or (C) 24 h after ConA injection ($n = 4$ per each time point). Immunohistochemical staining was conducted using anti-CD4, anti-CD11b, anti-Gr-1, and anti-F4/80 antibodies. Stained liver images shown are representative of three experiments performed. Magnification: ×100. Bars: 200 μm. (D) Quantification of $CD4^+$, $CD11b^+$, $Gr\text{-}1^+$, and $F4/80^+$ cells in four visual fields per ×100 low-power field in the liver of representative mice from each group. Data are shown as mean +SE ($n = 4$) and are representative of three experiments performed. $^*p < 0.05$, $^{**}p < 0.01$, $^{***}p < 0.005$, $^{****}p < 0.001$; Student's *t*-test. n.s.: not significant.

hours later, hepatic inflammatory cells were isolated and incubated with FITC-labeled anti-mouse CD11b (Beckman Coulter) and PE-labeled anti-mouse Gr-1 (Miltenyi Biotec) antibodies. The $CD11b^+Gr\text{-}1^+$ population was collected using a FACSAira II™ (Becton Dickinson). $CD11b^+Gr\text{-}1^+$ cells (1×10^5), which had been irradiated with 2000 rads, were co-cultured with 1×10^5 purified splenic T cells isolated from C57BL/6J mice in RPMI1640 medium (Invitrogen) supplemented with 10% heat-inactivated FBS, 1% antibiotic–antimycotic solution (Life Technologies), and ConA (4 μg/mL) for 48 h ($n = 4$). The culture was pulsed with [3H]thymidine (1 μCi/well) for 16 h and harvested. Thymidine incorporation was measured using a beta-counter (PerkinElmer, Waltham, MA, USA).

NO assay

C57BL/6J female mice were injected with 300 μg of ConA. Three hours later, 1×10^5 ADSCs were injected via the tail vein. After a further 3 h, hepatic inflammatory cells were isolated from ConA hepatitis mice with or without ADSC treatment ($n = 3$ each) and incubated in PBS supplemented with 2% BSA, PE-labeled anti-mouse Gr-1 antibody, and allophycocyanin-labeled anti-mouse CD11b antibody. Cells were then incubated in PBS containing 2.5 mg/mL diaminofluorescein-FM diacetate (Sekisui Medical Co., Ltd., Tokyo, Japan), which emits fluorescence at 515 nm in a reaction with NO, at 37°C for 30 min and subjected to FACS analysis using a FACSCalibur flow cytometer.

Arginase assay

Female C57BL/6J mice were injected with 300 μg of ConA. Three hours later, 1×10^5 ADSCs were injected via the tail vein. After further 3 h, hepatic inflammatory cells were isolated from ConA hepatitis mice with or without ADSC treatment ($n = 3$ each) and were lysed with PBS containing 10 mM Tris-HCl (pH 7.4) and 0.4% Triton X-100, supplemented with the proteinase inhibitor cocktail, cOmplete, Mini, EDTA-free® (Roche, Basel, Switzerland). One hundred micrograms of the lysis aliquot obtained were subject to an arginase activity assay using a QuantiChrom™ Arginase Assay kit (BioAssay Systems, Hayward, CA), which measures urea produced from the substrate, in accordance with the manufacturer's protocol.

Statistical analysis

All data are expressed as means ± SE. Statistical analyses were performed using the JMP software (ver.9.02; SAS Institute Japan Inc., Tokyo, Japan). Student's *t*-test and Wilcoxon signed-rank test were used. p values < 0.05 were considered to indicate statistical significance.

Acknowledgements: This study was supported, in part, by subsidies from the Japanese Ministry of Education, Culture, Sports, Science, and Technology and the Japanese Ministry of Health, Labor, and Welfare.

Conflict of interest: The authors declare no financial or commercial conflict of interest.

References

1 Zuk, P. A., Zhu, M., Ashjian, P., De Ugarte, D. A., Huang, J. I., Mizuno, H., Alfonso, Z. C. et al., Human adipose tissue is a source of multipotent stem cells. *Mol. Biol. Cell* 2002. **13**: 4279–4295.

2 Chamberlain, G., Fox, J., Ashton, B. and Middleton, J., Concise review: mesenchymal stem cells: their phenotype, differentiation capacity, immunological features, and potential for homing. *Stem Cells* 2007. **25**: 2739–2749.

3 Perez-Cano, R., Vranckx, J. J., Lasso, J. M., Calabrese, C., Merck, B., Milstein, A. M., Sassoon, E. et al., Prospective trial of adipose-derived regenerative cell (ADRC)-enriched fat grafting for partial mastectomy defects: the RESTORE-2 trial. *Eur. J. Surg. Oncol.* 2012. **38**: 382–389.

4 Janssens, S., Stem cells in the treatment of heart disease. *Annu. Rev. Med.* 2010. **61**: 287–300.

5 Hoogduijn, M. J., Popp, F., Verbeek, R., Masoodi, M., Nicolaou, A., Baan, C. and Dahlke, M. H., The immunomodulatory properties of mesenchymal stem cells and their use for immunotherapy. *Int. Immunopharmacol.* 2010. **10**: 1496–1500.

6 Baroni, G. S., Pastorelli, A., Manzin, A., Benedetti, A., Marucci, L., Solforosi, L., Di Sario, A. et al., Hepatic stellate cell activation and liver fibrosis are associated with necroinflammatory injury and Th1-like response in chronic hepatitis C. *Liver* 1999. **19**: 212–219.

7 Cerny, A. and Chisari, F. V., Pathogenesis of chronic hepatitis C: immunological features of hepatic injury and viral persistence. *Hepatology* 1999. **30**: 595–601.

8 Gershwin, M. E., Ansari, A. A., Mackay, I. R., Nakanuma, Y., Nishio, A., Rowley, M. J. and Coppel, R. L., Primary biliary cirrhosis: an orchestrated immune response against epithelial cells. *Immunol. Rev.* 2000. **174**: 210–225.

9 Krawitt, E. L., Autoimmune hepatitis. *N. Engl. J. Med.* 1996. **334**: 897–903.

10 Fujii, H. and Kawada, N., Inflammation and fibrogenesis in steatohepatitis. *J. Gastroenterol.* 2012. **47**: 215–225.

11 Dienes, H. P. and Drebber, U., Pathology of immune-mediated liver injury. *Dig. Dis.* 2010. **28**: 57–62.

12 Dai, L. J., Li, H. Y., Guan, L. X., Ritchie, G. and Zhou, J. X., The therapeutic potential of bone marrow-derived mesenchymal stem cells on hepatic cirrhosis. *Stem Cell Res.* 2009. **2**: 16–25.

13 Sanders, D. A., Moothoo, D. N., Raftery, J., Howard, A. J., Helliwell, J. R. and Naismith, J. H., The 1.2 A resolution structure of the Con A-dimannose complex. *J. Mol. Biol.* 2001. **310**: 875–884.

14 Kato, M., Ikeda, N., Matsushita, E., Kaneko, S. and Kobayashi, K., Involvement of IL-10, an anti-inflammatory cytokine in murine liver injury induced by concanavalin A. *Hepatol. Res.* 2001. **20**: 232–243.

15 **Kubo, N., Narumi, S., Kijima, H., Mizukami, H., Yagihashi, S., Hakamada, K. and Nakane, A.**, Efficacy of adipose tissue-derived mesenchymal stem cells for fulminant hepatitis in mice induced by concanavalin A. *J. Gastroenterol. Hepatol.* 2012. **27**: 165–172.

16 **Murdoch, C., Muthana, M., Coffelt, S. B. and Lewis, C. E.**, The role of myeloid cells in the promotion of tumour angiogenesis. *Nat. Rev. Cancer* 2008. **8**: 618–631.

17 **Banas, A., Teratani, T., Yamamoto, Y., Tokuhara, M., Takeshita, F., Quinn, G., Okochi, H. et al.**, Adipose tissue-derived mesenchymal stem cells as a source of human hepatocytes. *Hepatology* 2007. **46**: 219–228.

18 **Kaneko, Y., Harada, M., Kawano, T., Yamashita, M., Shibata, Y., Gejyo, F., Nakayama, T. et al.**, Augmentation of Valpha14 NKT cell-mediated cytotoxicity by interleukin 4 in an autocrine mechanism resulting in the development of concanavalin A-induced hepatitis. *J. Exp. Med.* 2000. **191**: 105–114.

19 **Tiegs, G., Hentschel, J. and Wendel, A.**, A T cell-dependent experimental liver injury in mice inducible by concanavalin A. *J. Clin. Invest.* 1992. **90**: 196–203.

20 **Halder, R. C., Aguilera, C., Maricic, I. and Kumar, V.**, Type II NKT cell-mediated anergy induction in type I NKT cells prevents inflammatory liver disease. *J. Clin. Invest.* 2007. **117**: 2302–2312.

21 **Schwabe, R. F. and Brenner, D. A.**, Mechanisms of liver injury. I. TNF-alpha-induced liver injury: role of IKK, JNK, and ROS pathways. *Am. J. Physiol. Gastrointest. Liver Physiol.* 2006. **290**: G583–G589.

22 **Schumann, J., Wolf, D., Pahl, A., Brune, K., Papadopoulos, T., van Rooijen, N. and Tiegs, G.**, Importance of Kupffer cells for T-cell-dependent liver injury in mice. *Am. J. Pathol.* 2000. **157**: 1671–1683.

23 **Clegg, C. H., Rulffes, J. T., Wallace, P. M. and Haugen, H. S.**, Regulation of an extrathymic T-cell development pathway by oncostatin M. *Nature* 1996. **384**: 261–263.

24 **Constant, S. L. and Bottomly, K.**, Induction of Th1 and Th2 CD4+ T cell responses: the alternative approaches. *Annu. Rev. Immunol.* 1997. **15**: 297–322.

25 **Contento, R. L., Molon, B., Boularan, C., Pozzan, T., Manes, S., Marullo, S. and Viola, A.**, CXCR4-CCR5: a couple modulating T cell functions. *Proc. Natl. Acad. Sci. USA* 2008. **105**: 10101–10106.

26 **Ponte, A. L., Marais, E., Gallay, N., Langonne, A., Delorme, B., Herault, O., Charbord, P. et al.**, The in vitro migration capacity of human bone marrow mesenchymal stem cells: comparison of chemokine and growth factor chemotactic activities. *Stem Cells* 2007. **25**: 1737–1745.

27 **Kushiyama, T., Oda, T., Yamada, M., Higashi, K., Yamamoto, K., Oshima, N., Sakurai, Y. et al.**, Effects of liposome-encapsulated clodronate on chlorhexidine gluconate-induced peritoneal fibrosis in rats. *Nephrol. Dial. Transplant.* 2011. **26**: 3143–3154.

Abbreviations: **ADSC**: adipose tissue derived stromal stem cell · **ALT**: alanine transferase · **LDH**: lactate dehydrogenase · **MDSC**: myeloid-derived suppressor cell · **MSC**: mesenchymal stromal stem cell

Full correspondence: Dr. Shuichi Kaneko, Disease Control and Homeostasis, Kanazawa University, 13-1 Takara-machi, Kanazawa, Ishikawa 920-8641, Japan
Fax: +81-76-234-4250
e-mail: skaneko@m-kanazwa.jp

Received: 17/3/2013
Revised: 3/7/2013
Accepted: 6/8/2013
Accepted article online: 12/8/2013

HEPATOLOGY
Official Journal of the American Association for the Study of Liver Diseases

LIVER INJURY/REGENERATION

Adipose Tissue-Derived Stem Cells as a Regenerative Therapy for a Mouse Steatohepatitis-Induced Cirrhosis Model

Akihiro Seki,[1,2*] Yoshio Sakai,[1,3*] Takuya Komura,[2] Alessandro Nasti,[2] Keiko Yoshida,[2] Mami Higashimoto,[2] Masao Honda,[1] Soichiro Usui,[2] Masayuki Takamura,[2] Toshinari Takamura,[2] Takahiro Ochiya,[4] Kengo Furuichi,[5] Takashi Wada,[3] and Shuichi Kaneko[1,2]

Cirrhosis is a chronic liver disease that impairs hepatic function and causes advanced fibrosis. Mesenchymal stem cells have gained recent popularity as a regenerative therapy since they possess immunomodulatory functions. We found that injected adipose tissue-derived stem cells (ADSCs) reside in the liver. Injection of ADSCs also restores albumin expression in hepatic parenchymal cells and ameliorates fibrosis in a nonalcoholic steatohepatitis model of cirrhosis in mice. Gene expression analysis of the liver identifies up- and down-regulation of genes, indicating regeneration/repair and anti-inflammatory processes following ADSC injection. ADSC treatment also decreases the number of intrahepatic infiltrating CD11b$^+$ and Gr-1$^+$ cells and reduces the ratio of CD8$^+$/CD4$^+$ cells in hepatic inflammatory cells. This is consistent with down-regulation of genes in hepatic inflammatory cells related to antigen presentation and helper T-cell activation. *Conclusion*: These results suggest that ADSC therapy is beneficial in cirrhosis, as it can repair and restore the function of the impaired liver. (HEPATOLOGY 2013;58:1133-1142)

Cirrhosis is a serious, life-threatening advanced stage of chronic liver disease that leads to hepatic dysfunction.[1] Cirrhosis frequently develops into hepatocellular carcinoma,[2,3] which exacerbates the prognosis of patients with cirrhosis. The ultimate treatment for cirrhosis is a liver transplant,[4] which can be lethal.[5] The number of donor livers, however, is not sufficient to meet the needs of all transplant patients. Thus, a novel therapy for cirrhosis needs to be developed to improve cirrhotic liver prognosis.

The underlying pathogenesis of chronic liver disease is persistent inflammation. Advanced disease is marked by advanced fibrosis concomitant with distorted liver architecture characterized by regenerative nodules and impaired hepatic function. Advanced fibrosis in the cirrhotic liver is also a risk factor for the development of hepatocellular carcinoma.[6] Treatment of cirrhosis suppresses inflammation by eradicating hepatitis virus infection or reducing liver steatosis in nonalcoholic steatohepatitis (NASH). Decreasing liver inflammation and restoring hepatocyte function improves the prognosis.

Pluripotent mesenchymal stem cells (MSCs) differentiate into adipocyte, chondrocyte, and osteocyte lineages.[7] These cells can also differentiate into other lineages, including neurons[8] and hepatocytes.[9,10] MSCs can also regulate the immune response.[11] Thus, MSCs attract attention as a therapeutic target in the

Abbreviations: ADSCs, adipose-tissue-derived stem cells; AFP, alpha-fetoprotein; Ath+HF, atherogenic high-fat; IL, interleukin; MMP, matrix metalloproteinase; MSC, mesenchymal stem cells; NASH, nonalcoholic steatohepatitis; PBS, phosphate-buffered saline; 18S rRNA, 18S ribosomal RNA; α-SMA, alpha-smooth muscle actin.

From the [1]Department of Gastroenterology, Kanazawa University Hospital, Ishikawa, Japan; [2]Disease Control and Homeostasis, Kanazawa University, Ishikawa, Japan; [3]Department of Laboratory Medicine, Kanazawa University Hospital, Ishikawa, Japan; [4]National Cancer Research Institute, Tokyo, Japan; [5]Division of Blood Purification, Kanazawa University Hospital, Ishikawa, Japan.

Received September 27, 2012; accepted April 15, 2013.

Supported in part by subsidies from the Japanese Ministry of Education, Culture, Sports, Science and Technology and the Japanese Ministry of Health, Labor and Welfare.

**These authors contributed equally to this work.*